Supplement of Atmos. Chem. Phys., 22, 8951–8971, 2022
https://doi.org/10.5194/acp-22-8951-2022-supplement

Atmospheric Chemistry and Physics Open Access

Supplement of

Budget of nitrous acid (HONO) at an urban site in the fall season of Guangzhou, China

Yihang Yu et al.

Correspondence to: Peng Cheng (chengp@jnu.edu.cn)

The introduction of the custom-built LOPAP

The LOPAP instrument was first developed by Heland et al. (2001), which is based on wet chemical sampling and photometric detection. Ambient air is sampled into an external sampling unit consisting of two similar stripping coils in series. Almost all the HONO and a small fraction of interfering substances (PAN, HNO_3, NO_2, etc.) are absorbed in solution in the first stripping coil, while in the second stripping coil only the interfering species are absorbed. To minimize the potential interferences, we assume the interferences absorbed in the first and the second coil are the same, so the real HONO concentration in the atmosphere is determined by subtracting the measured signal of the second coil from the measured signal of the first coil. The absorption solution R1 is a mixture reagent of 1 L hydrochloric acid (HCl) (37% volume fraction) and 100 g sulfanilamide dissolved in 9 L pure water. The dye solution R2, 2 g n-(1-naphtyl)-ethylendiamine-dihydrchloride (NEDA) dissolved in 10 L pure water, is then reacted with the absorption solution from two stripping coils pumped by a peristaltic pump to form colored azo dye. The light-absorbing colored azo dye is then pumped through a debubbler by the peristaltic pump and flows into the detection unit, which consists of two liquid waveguide capillary cells (World Precision Instrument, LWCC), one LED light source (Ocean Optics), two miniature spectrometers (Ocean Optics, Maya2000Pro) and several optical fibers. To correct for the small zero-drifts in the instrument's baseline, the zero measurements were conducted every 12 h by introducing zero air (highly pure nitrogen). During the instrument's operation, the instrument calibration was performed every week using the standard sodium nitrite ($NaNO_2$) solution (with the concentrations of 1–20 ppb, corresponding to atmospheric HONO mixing ratios of 0.245–4.9 ppbv).

Detection limit is defined as 3σ of HONO concentration measured in zero air. The detection limit of 5 pptv for this campaign was determined by zero air measurement. The precision (2σ) of the custom-build LOPAP is defined in this work as the minimum detectable change of a measured signal (Villena et al., 2011) and amounts to approximately 1.0% of 10 ppb nitrite concentrations (median value of observed ambient HONO concentrations). Time response is defined as the time interval between HONO signal decreases from 90% of the signal when start zero air running to 10% higher than the zero signal. It also relates to the liquid flow. The determined time response during the campaign is about 4 min considering the air flow of 1 L min^{-1} and liquid flow of 0.4 mL min^{-1}. Measurement error is the sum of statistic error and systematic error. Statistic error is defined as 1σ of HONO signal in zero air measurement. Systematic error is coming from the uncertainties of air flow rate, liquid flow rate and calibration factor, and is about 8% of measured HONO by applying "Gaussian Error Propagation" method (Trebs et al., 2004). The instrument parameters are listed in Table S1.

A commercial LOPAP (QUMA, Germany) operated by the Guangzhou Institute of Geochemistry Chinese Academy of Sciences (GIGCAS) also measured HONO during the observation. Unfortunately, only less than 10 days data were obtained by the commercial LOPAP due to malfunction. Our custom-built LOPAP was validated against the commercial LOPAP instrument with good agreement ($R^2 = 0.910$) (see Fig. S2), which further demonstrated the reliability of our instrument.

The evaluation of the interferences caused by other NOy species on NO_2 measurement using molybdenum converter

Our site is a typical urban site with heavy traffic emissions, as indicated by high concentrations of NO and NOx. Meanwhile, the average concentration of HONO, gaseous HNO_3 and particulate nitrate during the campaign were 0.74 ± 0.70 ppbv, 2.1 ± 2.0 ppbv and 4.2 ± 5.8 μg m^{-3}, respectively. PAN was not measured and is estimated around 0.84 ppbv based on earlier data at Guangzhou (Wang et al., 2015a) and the other NOy species can be ignored. Based on these, we roughly estimate the relative interferences of NOz (NOy-NOx) to NO_2 to be around 10%.

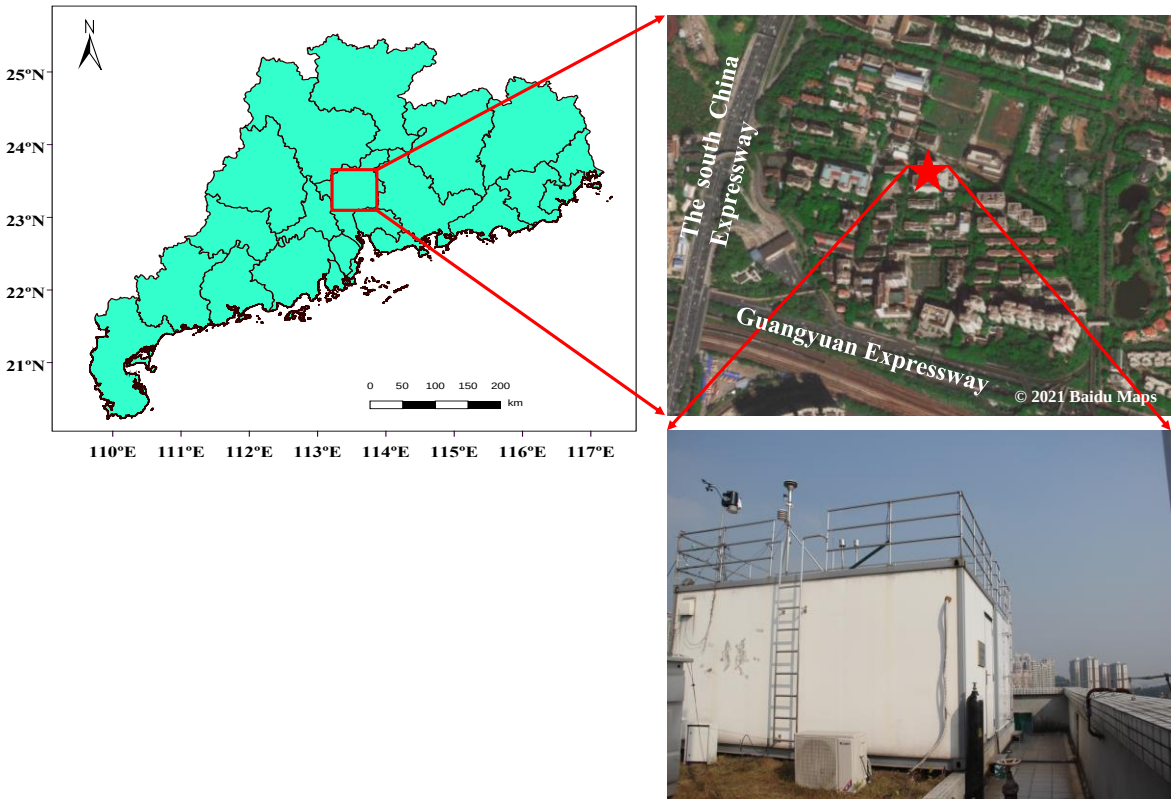

Figure S1. Schematic map of the measurement site in Guangzhou. The red star represents specimen building of the Guangzhou Institute of Geochemistry, Chinese Academy of Sciences (GIGCAS).

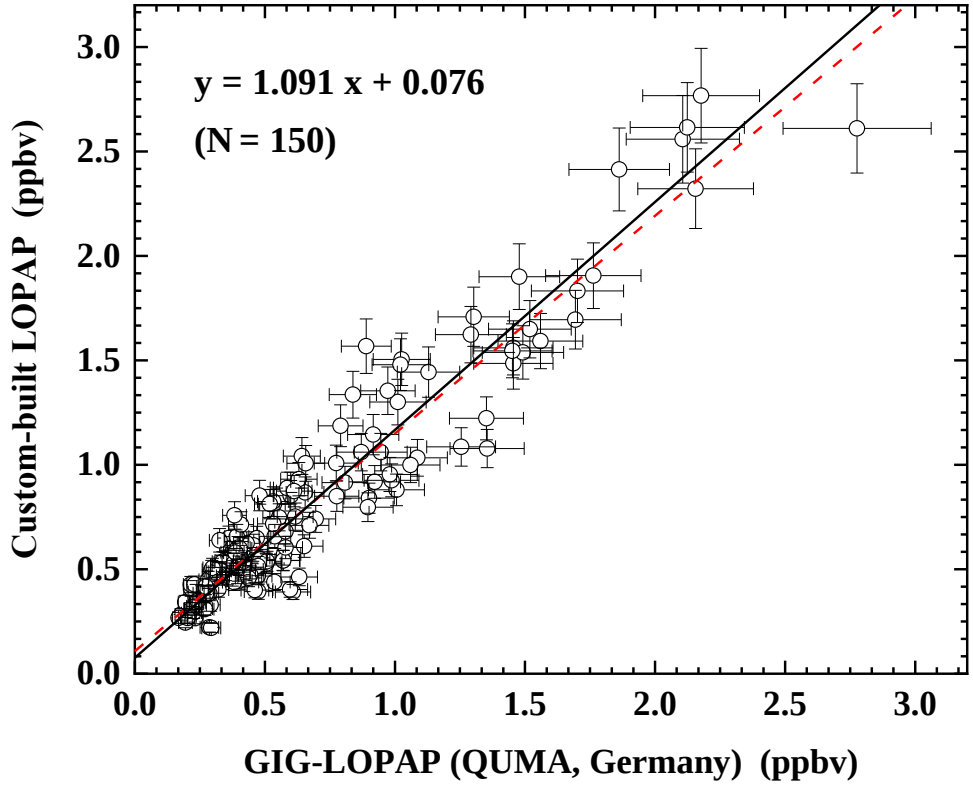

Figure S2. Intercomparison between the custom-built LOPAP with the commercial LOPAP (QUMA, Germany). The solid line denotes the linear fitting results with the "bivariate" method (slope: 1.091 ± 0.026, intercept: 0.076 ± 0.030), while the dashed line denotes that with the "standard" method (slope: 1.042 ± 0.027, intercept: 0.108 ± 0.022, R^2 = 0.910). The error bars represent the uncertainties of the custom-built LOPAP (8% + 5 pptv) and commercial LOPAP data (QUMA, Germany) (10% + 7 pptv). The HONO data from October 15–18 and November 1–6, 2018 was used for comparison.

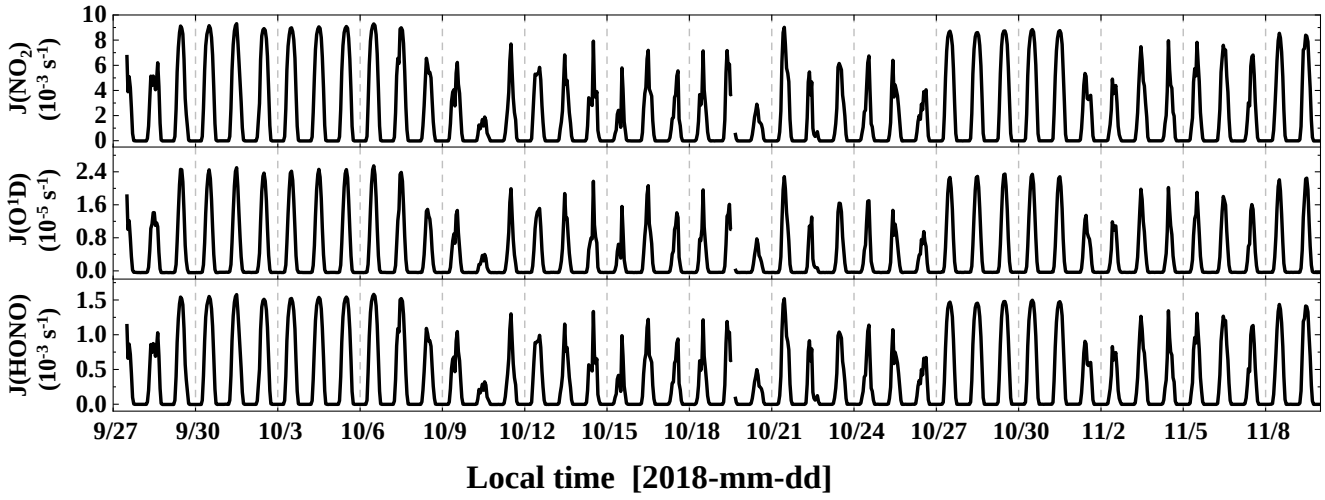

Figure S3. Temporal variations of photolysis rates J(HONO), J(O^1D) and J(NO_2) during the observation period.

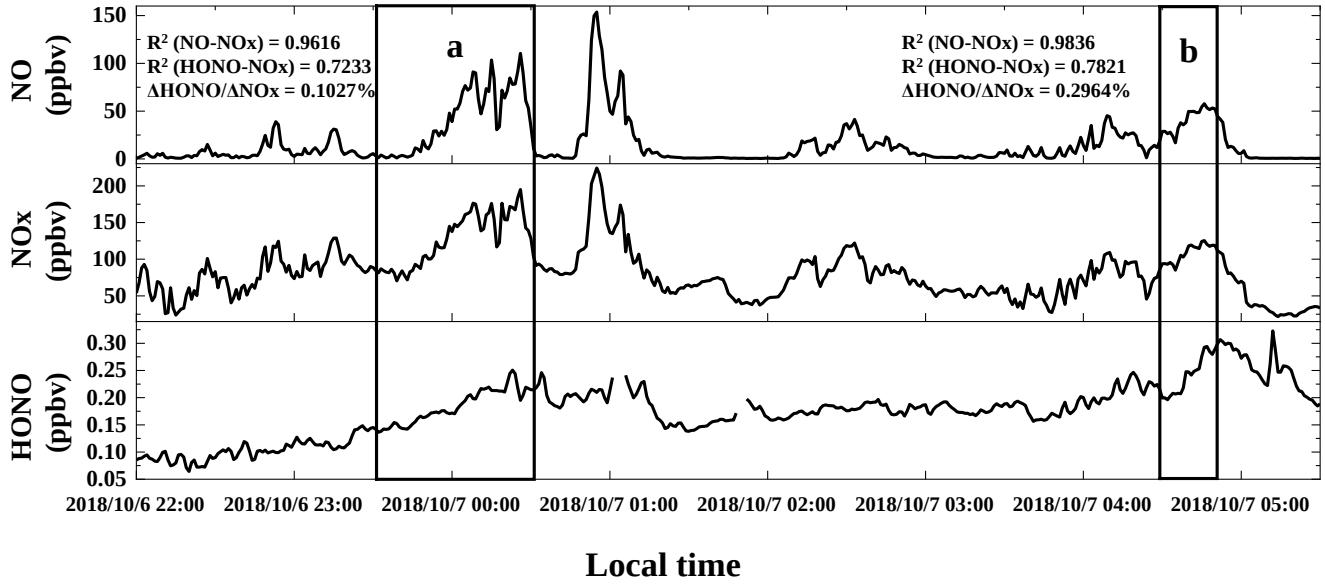

Figure S4. Temporal variations of nocturnal HONO, NOx and NO on October 6–7, 2018. The HONO emission factors were obtained according to the data in the black frames a and b.

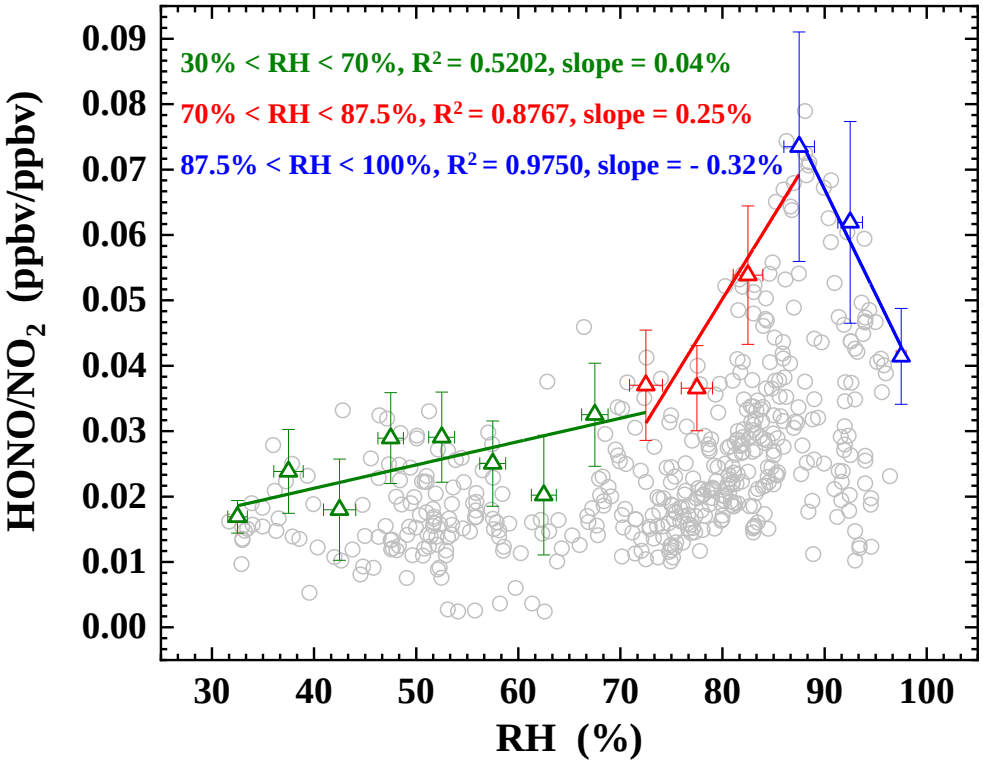

Figure S5. Scatter plot of HONO/NO_2 ratio against RH during nighttime from 18:00 to 6:00. Triangles are the average of top-5 HONO/NO_2 values in each 5% RH interval.

85

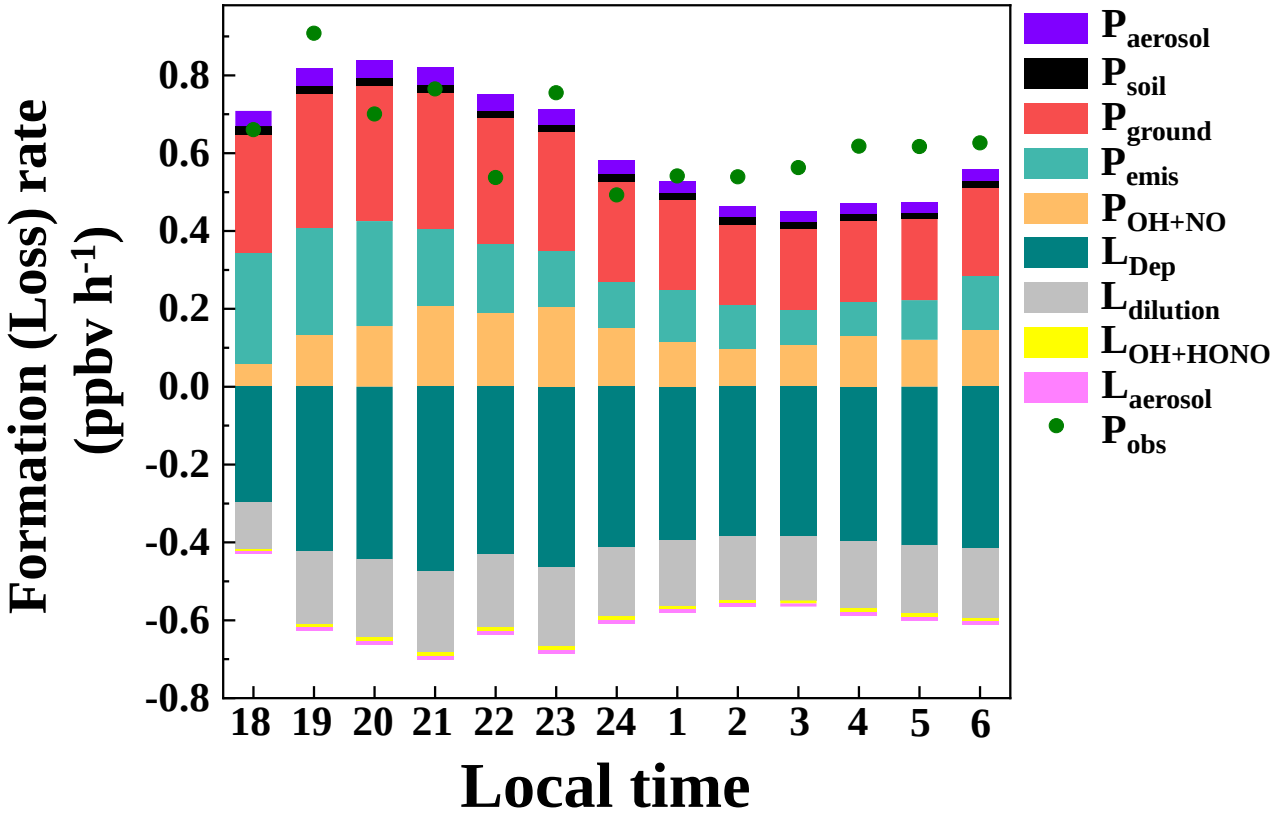

Figure S6. Nighttime HONO budget in Guangzhou during the observation period.

Table S1. The parameters of the custom-built LOPAP.

Parameters	Values
Air flow	1 L min^{-1}
Liquid flow	0.4 mL min^{-1}
Length of LWCC	100 cm
Detection limit	5 pptv
Detection range	5 pptv–10 ppbv
Time response	4 min
Uncertainty	8%

Table S2. Emission factors (ΔHONO/ΔNOx) and other information in 11 fresh plumes.

Starting time	Duration (min)	R^2 (NO-NOx)	R^2 (HONO-NOx)	ΔNO/ΔNOx	HONO/NOx	ΔHONO/ΔNOx
2018/10/6 23:29	62	0.9616	0.7233	0.90	0.002	0.001
2018/10/7 4:29	22	0.9836	0.7821	0.97	0.002	0.003
2018/10/7 20:44	34	0.9559	0.7054	0.88	0.011	0.010
2018/10/7 22:49	22	0.9904	0.8051	1.05	0.013	0.008
2018/10/20 0:33	24	0.9621	0.7826	0.96	0.020	0.007
2018/10/21 6:28	40	0.9959	0.9403	0.89	0.021	0.014
2018/10/25 6:55	20	0.9615	0.7291	1.04	0.024	0.014
2018/11/4 19:04	22	0.9761	0.8148	1.05	0.022	0.011
2018/11/4 22:01	78	0.9892	0.7684	1.02	0.016	0.007
2018/11/6 7:31	29	0.9835	0.7902	1.03	0.029	0.009
2018/11/7 4:56	30	0.9750	0.7007	0.93	0.027	0.015

Table S3. The overview of percentage of nighttime primary emissions of HONO from urban sites in China.

Location	Date	Nighttime NOx (ppbv)	$[HONO]_{emis}/[HONO]$ (%)	Emission ratio HONO/NOx (%)	Reference
Guangzhou	Oct 2015	57.9	15.1	0.65	1
Guangzhou	Sep–Nov 2018	47.7	47	0.9	2
Shanghai	May 2016	–	12.5	0.65	3
Changzhou	Apr 2017	–	31.4	0.69	4
Zhengzhou	Jan 2019	41	17[a]	0.65	5
		68.7	16[b]		
		107.3	16[c]		
Ji'nan	Nov 2013–Jan 2014	–	42	0.58	6
Ji'nan	Sep–Nov 2015	38	18	0.53	7
	Dec 2015–Feb 2016	78.5	21		
	Mar–May 2016	47.3	12		
	Jun–Aug 2016	29.1	15		
Beijing	Jan–Feb 2007	–	20.59	0.65	8
	Aug 2007	–	11.68		
Beijing	Oct–Nov 2014	94.5	39.6	0.65	9
Beijing	Dec 2015	–	48.8	0.8	10
Beijing	Dec 2015	–	52[b]	1.3	11
		–	40[c]		
Beijing	Dec 2016	–	29.3	0.78	12
Beijing	Aug–Sep 2018	–	17.6	0.8	13
Beijing	May–Jul 2018	–	14.21	0.78	14
	Nov 2018–Jan 2019	–	30.79		

[a]: clean; [b]: polluted; [c]: severely polluted. Reference: 1: Tian et al. (2018); 2: This work; 3: Cui et al. (2018); 4: Shi et al. (2020); 5: Hao et al. (2020); 6: Wang et al. (2015b); 7: Li et al. (2018); 8: Spataro et al. (2013); 9: Tong et al. (2015); 10: Tong et al. (2016); 11: Zhang et al. (2019); 12: Meng et al. (2020); 13: Jia et al. (2020); 14: Liu et al. (2021).

Table S4. The OH concentration is assumed of 0.5×10^6 molecules cm^{-3}. The integrated P^{net}_{OH+NO} of homogeneous reaction of NO + OH from 18:00 to 6:00.

OH/molecules cm^{-3}	Integrated P^{net}_{OH+NO}/ppbv	Measured HONO/ppbv
1×10^5	0.32	0.26
5×10^5	1.62	
1×10^6	3.24	

Table S5. Parameterisations of HONO production and loss mechanisms.

Mechanism	Parameterisation				Reference
	HONO formation/loss reactions	Median	Lower	Upper	
Primary emission		P_{emis} = 0.16 ppbv h^{-1}	Emission source inventory 1	Emission source inventory 2	1
NO + OH	NO + OH → HONO	OH = 0.5 × 10^6 cm^{-3}	1.0 × 10^5 cm^{-3}	1.0 × 10^6 cm^{-3}	2
NO_2 on aerosol	NO_2 + aerosol → HONO	$\gamma_{NO_2 \rightarrow aerosol}$ = 4 × 10^{-6}	2 × 10^{-7}	1 × 10^{-5}	3, 4, 5
NO_2 on ground	NO_2 + ground → HONO	$\gamma_{NO_2 \rightarrow ground}$ = 4 × 10^{-6}	2 × 10^{-7}	1 × 10^{-5}	3, 4, 5
Soil emission		water content: 35%–45%	45%–55%	25%–35%	6, 7, 8
Deposition		V_d = 2.5 cm s^{-1}	0.077 cm s^{-1}	3 cm s^{-1}	9, 10, 11,12
Vertical transport		$k_{(dilution)}$ = 0.23 h^{-1}	0.1 h^{-1}	0.44 h^{-1}	13, 14, 15
HONO on aerosol		$\gamma_{HONO \rightarrow aerosol}$ = 4 × 10^{-5}	3 × 10^{-7}	5 × 10^{-4}	16, 17, 18
HONO + OH	HONO + OH → NO_2 + H_2O	OH = 0.5 × 10^6 cm^{-3}	1.0 × 10^5 cm^{-3}	1.0 × 10^6 cm^{-3}	2

Emission source inventory 1 denotes the 2017 NOx emission source inventory of Guangzhou city; Emission source inventory 2 denotes the 2017 NOx emission source inventory of the 3 km × 3 km grid cell centred on the Guangzhou Institute of Geochemistry. Reference: 1: Huang et al. (2021); 2: Tan et al. (2019); 3: Li et al. (2018); 4: Liu et al. (2019); 5: Zhang et al. (2021); 6: Oswald et al. (2013); 7: Liu et al. (2020a); 8: Liu et al. (2020b); 9: Stutz et al. (2002); 10: Harrison and Kitto (1994); 11: Harrison et al. (1996); 12: Spindler et al. (1999); 13: Dillon et al. (2002); 14: Lin et al. (1996); 15: Kalthoff et al. (2000); 16: El Zein et al. (2013); 17: El Zein and Bedjanian (2012); 18: Romanias et al. (2012).

References

Cui, L., Li, R., Zhang, Y., Meng, Y., Fu, H., and Chen, J.: An observational study of nitrous acid (HONO) in Shanghai, China: The aerosol impact on HONO formation during the haze episodes, Science of The Total Environment, 630, 1057-1070, https://doi.org/10.1016/j.scitotenv.2018.02.063, 2018.

Dillon, M. B., Lamanna, M. S., Schade, G. W., Goldstein, A. H., and Cohen, R. C.: Chemical evolution of the Sacramento urban plume: Transport and oxidation, Journal of Geophysical Research: Atmospheres, 107, ACH 3-1-ACH 3-15, https://doi.org/10.1029/2001JD000969, 2002.

El Zein, A., and Bedjanian, Y.: Reactive Uptake of HONO to TiO2 Surface: "Dark" Reaction, The Journal of Physical Chemistry A, 116, 3665-3672, https://doi.org/10.1021/jp300859w, 2012.

El Zein, A., Romanias, M. N., and Bedjanian, Y.: Kinetics and Products of Heterogeneous Reaction of HONO with Fe2O3 and Arizona Test Dust, Environmental Science & Technology, 47, 6325-6331, https://doi.org/10.1021/es400794c, 2013.

Hao, Q., Jiang, N., Zhang, R., Yang, L., and Li, S.: Characteristics, sources, and reactions of nitrous acid during winter at an urban site in the Central Plains Economic Region in China, Atmos. Chem. Phys., 20, 7087-7102, https://doi.org/10.5194/acp-20-7087-2020, 2020.

Harrison, R. M., and Kitto, A.-M. N.: Evidence for a surface source of atmospheric nitrous acid, Atmospheric Environment, 28, 1089-1094, https://doi.org/10.1016/1352-2310(94)90286-0, 1994.

Harrison, R. M., Peak, J. D., and Collins, G. M.: Tropospheric cycle of nitrous acid, Journal of Geophysical Research: Atmospheres, 101, 14429-14439, https://doi.org/10.1029/96JD00341, 1996.

Heland, J., Kleffmann, J., Kurtenbach, R., and Wiesen, P.: A New Instrument To Measure Gaseous Nitrous Acid (HONO) in the Atmosphere, Environmental Science & Technology, 35, 3207-3212, https://doi.org/10.1021/es000303t, 2001.

Huang, Z., Zhong, Z., Sha, Q., Xu, Y., Zhang, Z., Wu, L., Wang, Y., Zhang, L., Cui, X., Tang, M., Shi, B., Zheng, C., Li, Z., Hu, M., Bi, L., Zheng, J., and Yan, M.: An updated model-ready emission inventory for Guangdong Province by incorporating big data and mapping onto multiple chemical mechanisms, Science of The Total Environment, 769, 144535, https://doi.org/10.1016/j.scitotenv.2020.144535, 2021.

Jia, C., Tong, S., Zhang, W., Zhang, X., Li, W., Wang, Z., Wang, L., Liu, Z., Hu, B., Zhao, P., and Ge, M.: Pollution characteristics and potential sources of nitrous acid (HONO) in early autumn 2018 of Beijing, Science of The Total Environment, 735, 139317, https://doi.org/10.1016/j.scitotenv.2020.139317, 2020.

Kalthoff, N., Horlacher, V., Corsmeier, U., Volz-Thomas, A., Kolahgar, B., Geiß, H., Möllmann-Coers, M., and Knaps, A.: Influence of valley winds on transport and dispersion of airborne pollutants in the Freiburg-Schauinsland area, Journal of Geophysical Research: Atmospheres, 105, 1585-1597, https://doi.org/10.1029/1999JD900999, 2000.

Li, D., Xue, L., Wen, L., Wang, X., Chen, T., Mellouki, A., Chen, J., and Wang, W.: Characteristics and sources of nitrous acid in an urban atmosphere of northern China: Results from 1-yr continuous observations, Atmospheric Environment, 182, 296-306, https://doi.org/10.1016/j.atmosenv.2018.03.033, 2018.

Lin, X., Roussel, P. B., Laszlo, S., Taylor, R., Meld, O. T., Shepson, P. B., Hastie, D. R., and Niki, H.: Impact of Toronto urban emissions on ozone levels downwind, Atmospheric Environment, 30, 2177-2193, https://doi.org/10.1016/1352-2310(95)00130-1, 1996.

Liu, J., Liu, Z., Ma, Z., Yang, S., Yao, D., Zhao, S., Hu, B., Tang, G., Sun, J., Cheng, M., Xu, Z., and Wang, Y.: Detailed budget analysis of HONO in Beijing, China: Implication on atmosphere oxidation capacity in polluted megacity, Atmospheric Environment, 244, 117957, https://doi.org/10.1016/j.atmosenv.2020.117957, 2021.

Liu, Y., Lu, K., Li, X., Dong, H., Tan, Z., Wang, H., Zou, Q., Wu, Y., Zeng, L., Hu, M., Min, K. E., Kecorius, S., Wiedensohler, A., and Zhang, Y.: A Comprehensive Model Test of the HONO Sources Constrained to Field Measurements at Rural North China Plain, Environ Sci Technol, https://doi.org/10.1021/acs.est.8b06367, 2019.

Liu, Y., Ni, S., Jiang, T., Xing, S., Zhang, Y., Bao, X., Feng, Z., Fan, X., Zhang, L., and Feng, H.: Influence of Chinese New Year overlapping COVID-19 lockdown on HONO sources in Shijiazhuang, Science of The Total Environment, 745, 141025, https://doi.org/10.1016/j.scitotenv.2020.141025, 2020a.

Liu, Y., Zhang, Y., Lian, C., Yan, C., Feng, Z., Zheng, F., Fan, X., Chen, Y., Wang, W., Chu, B., Wang, Y., Cai, J., Du, W., Daellenbach, K. R., Kangasluoma, J., Bianchi, F., Kujansuu, J., Petäjä, T., Wang, X., Hu, B., Wang, Y., Ge, M., He, H., and Kulmala, M.: The promotion effect of nitrous acid on aerosol formation in wintertime in Beijing: the possible contribution of traffic-related emissions, Atmos. Chem. Phys., 20, 13023-13040, https://doi.org/10.5194/acp-20-13023-2020, 2020b.

Meng, F., Qin, M., Tang, K., Duan, J., Fang, W., Liang, S., Ye, K., Xie, P., Sun, Y., Xie, C., Ye, C., Fu, P., Liu, J., and Liu, W.: High-resolution vertical distribution and sources of HONO and NO_2 in the nocturnal boundary layer in urban Beijing, China, Atmos. Chem. Phys., 20, 5071-5092, https://doi.org/10.5194/acp-20-5071-2020, 2020.

Oswald, R., Behrendt, T., Ermel, M., Wu, D., Su, H., Cheng, Y., Breuninger, C., Moravek, A., Mougin, E., Delon, C., Loubet, B., Pommerening-Röser, A., Sörgel, M., Pöschl, U., Hoffmann, T., Andreae, M. O., Meixner, F. X., and Trebs, I.: HONO Emissions from Soil Bacteria as a Major Source of Atmospheric Reactive Nitrogen, Science, 341, 1233-1235, https://doi.org/10.1126/science.1242266, 2013.

Romanias, M. N., El Zein, A., and Bedjanian, Y.: Reactive uptake of HONO on aluminium oxide surface, Journal of Photochemistry and Photobiology A: Chemistry, 250, 50-57, https://doi.org/10.1016/j.jphotochem.2012.09.018, 2012.

Shi, X., Ge, Y., Zheng, J., Ma, Y., Ren, X., and Zhang, Y.: Budget of nitrous acid and its impacts on atmospheric oxidative capacity at an urban site in the central Yangtze River Delta region of China, Atmospheric Environment, 238, 117725, https://doi.org/10.1016/j.atmosenv.2020.117725, 2020.

Spataro, F., Ianniello, A., Esposito, G., Allegrini, I., Zhu, T., and Hu, M.: Occurrence of atmospheric nitrous acid in the urban area of Beijing (China), Science of The Total Environment, 447, 210-224, https://doi.org/10.1016/j.scitotenv.2012.12.065, 2013.

Spindler, G., Brüggemann, E., and Herrmann, H.: Nitrous acid (HNO_2) concentration measurements and estimation of dry deposition over grassland in eastern Germany, Proceedings of the EUROTRAC Symposium 1998, Vol. 2, WITpress, Southampton, UK, 218–222, 1999.

Stutz, J., Alicke, B., and Neftel, A.: Nitrous acid formation in the urban atmosphere: Gradient measurements of NO_2 and HONO over grass in Milan, Italy, Journal of Geophysical Research: Atmospheres, 107, 8192, https://doi.org/10.1029/2001JD000390, 2002.

Stutz, J., Alicke, B., Ackermann, R., Geyer, A., Wang, S., White, A. B., Williams, E. J., Spicer, C. W., and Fast, J. D.: Relative humidity dependence of HONO chemistry in urban areas, Journal of Geophysical Research: Atmospheres, 109, https://doi.org/10.1029/2003JD004135, 2004.

Tan, Z., Lu, K., Hofzumahaus, A., Fuchs, H., Bohn, B., Holland, F., Liu, Y., Rohrer, F., Shao, M., Sun, K., Wu, Y., Zeng, L., Zhang, Y., Zou, Q., Kiendler-Scharr, A., Wahner, A., and Zhang, Y.: Experimental budgets of OH, HO2, and RO2 radicals and implications for ozone formation in the Pearl River Delta in China 2014, Atmos. Chem. Phys., 19, 7129-7150, https://doi.org/10.5194/acp-19-7129-2019, 2019.

Tian, Z., Yang, W., Yu, X., Zhang, M., Zhang, H., Cheng, D., Cheng, P., and Wang, B.: HONO pollution characteristics and nighttime sources during autumn in Guangzhou, China Environmental Science, 39 (05), 2000-2009, https://doi.org/10.13227/j.hjkx.201709269, 2018.

Tong, S., Hou, S., Zhang, Y., Chu, B., Liu, Y., He, H., Zhao, P., and Ge, M.: Comparisons of measured nitrous acid (HONO) concentrations in a pollution period at urban and suburban Beijing, in autumn of 2014, Science China Chemistry, 58, 1393-1402, https://doi.org/10.1007/s11426-015-5454-2, 2015.

Tong, S., Hou, S., Zhang, Y., Chu, B., Liu, Y., He, H., Zhao, P., and Ge, M.: Exploring the nitrous acid (HONO) formation mechanism in winter Beijing: direct emissions and heterogeneous production in urban and suburban areas, Faraday Discuss, 189, 213-230, https://doi.org/10.1039/C5FD00163C, 2016.

Trebs, I., Meixner, F. X., Slanina, J., Otjes, R., Jongejan, P., and Andreae, M. O.: Real-time measurements of ammonia, acidic trace gases and water-soluble inorganic aerosol species at a rural site in the Amazon Basin, Atmos. Chem. Phys., 4, 967-987, https://doi.org/10.5194/acp-4-967-2004, 2004.

Villena, G., Bejan, I., Kurtenbach, R., Wiesen, P., and Kleffmann, J.: Development of a new Long Path Absorption Photometer (LOPAP) instrument for the sensitive detection of NO₂ in the atmosphere, Atmos. Meas. Tech., 4, 1663-1676, https://doi.org/10.5194/amt-4-1663-2011, 2011.

Wang, B. G., Zhu, D., Zou, Y., Wang, H., Zhou, L., Ouyang, X., Shao, H. F., and Deng, X. J.: Source analysis of peroxyacetyl nitrate (PAN) in Guangzhou, China: a yearlong observation study, Atmos. Chem. Phys. Discuss., 2015, 17093-17133, https://doi.org/10.5194/acpd-15-17093-2015, 2015a.

Wang, L., Wen, L., Xu, C., Chen, J., Wang, X., Yang, L., Wang, W., Yang, X., Sui, X., Yao, L., and Zhang, Q.: HONO and its potential source particulate nitrite at an urban site in North China during the cold season, Science of The Total Environment, 538, 93-101, https://doi.org/10.1016/j.scitotenv.2015.08.032, 2015b.

Zhang, S., Sarwar, G., Xing, J., Chu, B., Xue, C., Sarav, A., Ding, D., Zheng, H., Mu, Y., Duan, F., Ma, T., and He, H.: Improving the representation of HONO chemistry in CMAQ and examining its impact on haze over China, Atmos. Chem. Phys., 21, 15809-15826, https://doi.org/10.5194/acp-21-15809-2021, 2021.

Zhang, W., Tong, S., Ge, M., An, J., Shi, Z., Hou, S., Xia, K., Qu, Y., Zhang, H., Chu, B., Sun, Y., and He, H.: Variations and sources of nitrous acid (HONO) during a severe pollution episode in Beijing in winter 2016, Science of The Total Environment, 648, 253-262, https://doi.org/10.1016/j.scitotenv.2018.08.133, 2019.